

# Estimating Center of Pressure of a Bipedal Mechanism Using a Proprioceptive Artificial Skin around its Ankles

Darío Urbina-Meléndez<sup>1</sup>, Jiaoran Wang<sup>2</sup>, Daniel Wang<sup>2</sup>, Ali Marjaninejad<sup>1</sup> and Francisco J. Valero-Cuevas<sup>\*1,3</sup>

**Abstract**— Estimating the Center of Pressure (CoP) under legged robots is useful to control their posture and gait. This is traditionally done using contact sensors at the base of the foot or with sensors on distal joints, which are subject to wear and damage due to impulse forces. In vertebrates, skin and ligament deformation at the ankle is a particularly rich source of sensory information for locomotion. For our bipedal mechanism, afferent signals from sensors on synthetic skin wrapped around the ankles sufficed to estimate the location of the CoP with a mean accuracy  $>81.5\%$ . For this we used K-Nearest Neighbors (KNN) algorithm trained on the same force magnitude applied at four and nine ground-truth CoP locations. For a single mechanical foot (i.e., single stance), signals from skin or ligaments (i.e., elastic rubber sheets and cables, respectively) also sufficed to calculate the CoP (Mean prediction accuracy  $>91.3\%$ ). Moreover, the visco-elasticity of these elements serves to passively stabilize the ankle. Importantly, training the single leg case with forces of different magnitudes also resulted in similarly accurate mean CoP prediction accuracy  $>84.5\%$ . We show that using bio-inspired proprioceptive skins and/or ligament arrangements can provide reliable COP predictions, while permitting arbitrary postures of the ankle and no sensors on the sole of the foot prone to wear and damage. This novel approach to estimation of the CoP can be used to improve locomotion control in a new class of bio-inspired rigid, soft and hybrid (soft-rigid) legged robots.

## I. INTRODUCTION

In contrast to engineered systems where controlled variables are measured directly and accurately, biological systems use mechanoreceptors that are often distributed and non-collocated [1], [2]. Haptic sensors on the skin are often thought of as pressure sensors which help on estimating parameters like the Center of Pressure (CoP) on the soles of the feet [3], [4]. However, a less known but no less critical example of noncollocated sensors (both, in animals and in robots) is that of mechanoreceptors on the skin surrounding joints [5] [6]. These cutaneous sensors react to stretch rather than pressure and are a prime example where the information from multiple distributed mechanoreceptors are processed to extract estimates of joint angles which the nervous system

<sup>1</sup>D.U.-M, A.M. and F.V.-C are with Department of Biomedical Engineering, University of Southern California, Los Angeles, CA 90089 USA. [urbiname] [marjanin] [valero]@usc.edu

<sup>2</sup>J.W. and D.W. are with Department of Aerospace & Mechanical Engineering, University of Southern California, Los Angeles, CA 90089 USA. [jiaoranw] [danielzw] [valero]@usc.edu

<sup>3</sup>F.V.-C is also with Division of Biokinesiology and Physical Therapy, University of Southern California, Los Angeles, CA 90089 USA.

\*F.V.-C. is the corresponding author. valero@usc.edu

uses to control limb movements [7], [8], [9]. Furthermore, skin stretch plays an important role in understanding ankle positions [10], [11], [12]. Here we explored whether the strain measured by sensors on a low-cost artificial skin wrapped around the ankles of a bipedal mechanism suffices to estimate its CoP (Fig. 1).

Common solutions for measurement of the COP involve signal acquisition from the sole of the robot's foot, to then use a model-based, [13], [14], [15], [16], [17] or a data-driven approach [18]. For some of the mentioned studies, it is described that the sensors are used to calculate the Zero Moment Point (ZMP). For these studies, calculation of ZMP depends on the CoP location; the former should always coincide with the later for dynamically balanced configurations [19]. Relying on detailed models of the robot's dynamics to calculate the CoP makes the system prone to failure when there are mismatches between the model and the real system dynamics due to wear and tear, damage, degradation, lack of information about the system, model simplicity or poor parameter identification [20]. In [21] a “redundant” sensor architecture together with a model-free machine learning approach is used to observe the behaviour of a soft actuator. Similarly to [21], we use machine learning to avoid the need for precise modeling and characterization of sensors and body dynamics.

We calculate the position of the CoP by measuring the strain experienced by a low-cost sensorized artificial skin wrapped around the ankles of an eight Degrees-of-Freedom (DoF) biped, as well as around a two DoF uniped structure. This skin functions as a passive neutral-position ankle stabilizer while providing strain measurements as afferent sensory information. We used these strain measurements to train a K-Nearest Neighbor (KNN) algorithm to estimate the CoP's location known a priori. The foot-leg mechanism, stabilized by the taut elastic skin makes the ankle joints return to a neutral configuration when not loaded. To further validate our results, we also performed experiments where we substituted the skin with ligaments with different stiffnesses to operate like guy-wires. This approach presents an alternative to sensors on the sole of the foot which are subject to wear and potential damage due to impulse forces caused by robot-floor interaction [22].

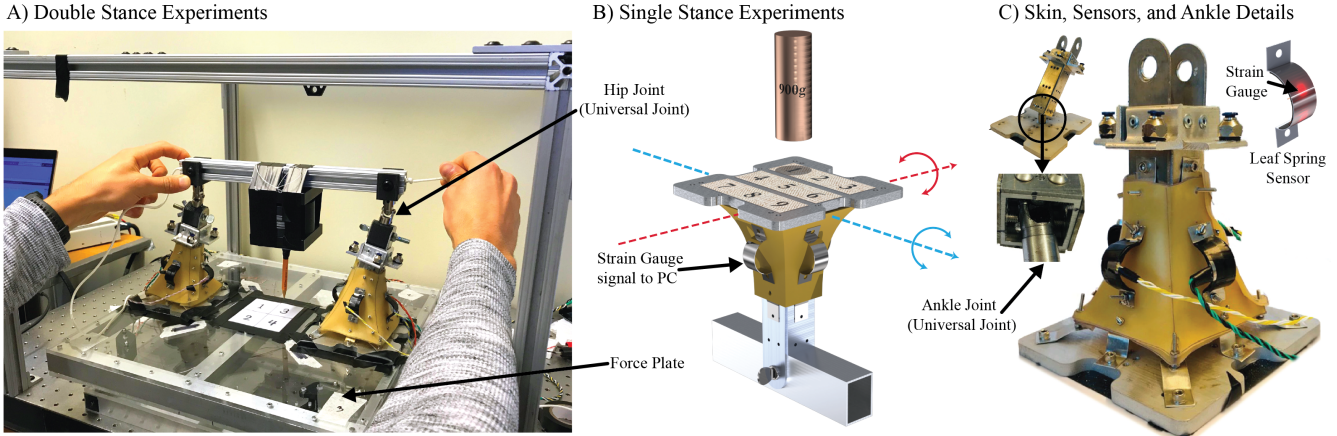


Fig. 1. **A and B show experiments to estimate the Center of Pressure, while C presents device details.** **A)** Biped standing on the force plate with CoP sensing area marked by a numbered grid. The force plate provides ground truth CoP locations (i.e., labels) while signals from four leaf spring sensors on each of the biped's ankles are recorded (i.e., features). **B)** Foot structure in an upside-down position to which Center of Pressure loads were applied to different locations on its sole. Simultaneously, data was recorded from the spring leaf sensors (i.e., features). **C)** Ankle joint consists of a universal joint. Two strain gauges are encapsulated inside two metal layers that form the leaf spring sensor. When the leaf spring geometry changes due to the skin elongation or contraction, the strain gauge electric resistance changes, generating a signal which depends on the strain the skin experiences derived from its elongation.

## II. METHODS

### A. Biped, Artificial Skin, Ligaments and Force Plate Construction

We developed a simple biped with eight DoF (i.e., two per ankle and two per hip joint), Fig. 1-A. For manufacture and debugging simplicity we did not include knees. As explained in [19], the forces and moments that an ankle is subjected to, can be used to understand foot-ground interaction; thus the shape of a structure over this joint can be ignored or, in our case simplified. The two legs are connected by a transversal post which we call "hip". We added a 900 grams mass (i.e., black cube in Fig 1-A) to the hip bar to increase the load and moments applied to the ground and ankle joints respectively. Due to the biped's symmetry with respect to its sagittal plane, and the high density of the 900 grams mass compared to the hip bar, we know that the Center of Mass (CoM) of the biped is located within this mass, for these experiments a different mass could have been used, as long as the biped's CoM location is the one just described. The leg and foot incorporates mounting points for both skin and ligament components (Fig. 1-C and 2).

We also created a sensorized visco-elastic skin structure. The sensing component of the skin, which we call "leaf spring sensor" consists of three parts: a strain device encapsulated in a double-layer aluminum arch, a load bearing buffer structure made of a double-layer of highly elastic rubber polymer, and metal connectors that facilitate the connection to the leg structure (Fig. 1-C, upper right corner). Two *Comidox BF120-3AA* strain gauges were attached to the proximal side of the arch structure and reinforced with an electrical tape infill. When the leg experiences a perturbation, the skin elongates causing the strain gauges to sense the surface deformation of the aluminum arch structures. A pair

of *Adafruit ADS-1015* amplifiers (Adafruit Industries, New York, NY, USA) were used in conjunction with a diagonal-half Wheatstone bridge to prepare the strain gauge signals for acquisition using a PC.

For some experiments, we replaced the skin or sections of it with ligaments (Fig. 2); to mount them, we created a structure employing *SparkFun TAL-220b* load cells (*SparkFun Electronics*, Boulder, CO, USA) as the sensing element. As ligaments, we used *Dacron®* cable and extension springs, and then used them to couple the load cells to the leg (Fig. 2). The flexibility and elasticity of these ligaments buffered the load cell from the motion of the leg. This was done to combat the typically limited range of motion of commercially available load cells. Four load cells and accompanying cable mounting mechanisms were attached to the leg structure and special care was taken to maintain equal tension on each load cell while the structure was in equilibrium. The consistent elastic properties of the ligaments (especially the extension springs version) combined with a stiff mounting structure allowed us to reliably measure load-cell tension, even after extensive use and testing.

To measure the ground truth of the CoP for the double stance case, we created a  $40.9 \times 40.9$  cm force plate sensor (Fig 1-A). The plate edges dimensions were chosen based on the biped's support polygon dimensions (i.e., three foot-sole areas). Four *SparkFun TAL-220b* load cells placed under the plate's surface, determined the  $8.0 \times 8.0$  cm CoP sensing area (i.e., square framed with black electrical tape in Fig 1-A). Placing the sensors in this position increased the sensitivity to the CoP position variations throughout experiments.

Overall, the mechanisms' manufacture was of low-cost, keeping in mind that we want to show that the introduced techniques can be applied to a variety of equivalent ankles and artificial skins incorporating different technologies.

### B. Double Stance Experiments

First, we trained the force plate on both nine and four ground truth CoP locations marked on a numbered  $8 \times 8$  cm grid on the plate center, subdivided by four or nine squares (16 and  $7.1 \text{ cm}^2$  respectively). For this, we used a mass equivalent to the mass of the biped but with a  $2.4 \text{ cm}^2$  base to ensure localized loading. We then centered the biped over the force plate and positioned its CoM centered over the numbered grid. We used the trained platform to assign CoP values (i.e., labels) to the afferent signals provided by the skin (i.e., features) while manually manipulating the biped mechanism to place its CoM over different locations of the numbered grid (Fig. 1-A). During the experiments, the CoM remained over each number in the grid for the same amount of time.

As shown in Fig. 1-A, to ensure that the load experienced by the platform only depends on the biped's position and mass, we equipped the bipedal structure with a rope to pull the hip towards a desired location, while we compensated rotational hip movements by holding the opposite side of the hip. Hip rotation compensation was done to keep the CoM projection on the force plate within the numbered grid area. In our experiments, CoP and CoM are in the same region (i.e., anterior or posterior with respect to the coronal plane, and/or lateral right or left with respect to the sagittal plane); this is consistent with the well-studied relationship between CoM and CoP for static cases [23], [24]. Due to the low friction between the metal foot and the acrylic platform, electrical tape was used to hold the foot at the desired position on the force plate.

The prediction of the CoP is possible after training a KNN algorithm [25] with afferent strain data from a synthetic skin (i.e., features), and using CoP locations as ground truth labels. We report results of five nearest neighbors ( $K = 5$ ). For some cases there is a better prediction accuracy using a different  $K$ , but considering that the best  $K$  cannot be determined while a robot operates, we chose  $K=5$  as our standard parameter for our algorithm.

### C. Single Stance Experiments

For this experiment, we mounted just one foot of the biped on an upside-down position. This allows its two degree-of-freedom ankle to flex when applying a 900 gram load. We first applied this load across nine numbered and equally segmented locations forming a  $3 \times 3$  grid of boxes on its upward facing sole. For a second experiment version, we increased the resolution of the square segments to 16, forming a  $4 \times 4$  grid on the sole. For both cases, the total grid area was  $85.9 \text{ cm}^2$ .

A 900 grams mass was used to mimic the load that our biped foot would experience while being on single stance position. Each sequence consisted of applying the load to all grid locations by a human operator following a visual cue on a screen, while data was recorded from the leaf spring sensors (i.e., features). The collected data consists of 28 complete sequences. (Fig. 1-B).



**Fig. 2. Non-homogeneously distributed sensors, subjected to different conditions can enable the prediction of body states.** A) Render of Foot-Ankle-Leg with Dacron Cable Ligament Assembly; ligaments can also be extension springs, as shown in B). Two mounting points are available, one being more proximal to the knee. When using the distal mounting point, we noticed a loss in state observability due to the universal joint and mount point alignment. B) Foot-Ankle-Leg with a combination of skin with 30 mm Leaf Springs and a Extension Spring Ligament.

In the same way as described for the double stance experiment, the prediction of the CoP is possible by using skin afferent information as features and CoP locations as labels to train a KNN algorithm [25]. The main difference is, in the case of the double stance, the ground truth CoP was given by a trained force plate. But, for the single stance experiment, the labels were automatically assigned. The operator follows a visual cue on a screen to apply the load to the foot sole. Same values shown on the screen are assigned as labels to the data features. While a value is shown on the screen, a batch of 25 lines of data are recorded (each line containing all sensors readings), only the twelfth line of each batch is used to train the KNN model. This helps to ensure that the recorded features corresponds to the correct ground truth CoP label, by giving enough time to the operator to manually change the position of the load to the correspondent value on the foot sole grid.

### D. Code

For Sections II-B and II-C We used C++ (Arduino boards) and Mathworks (Natick, MA, USA) MATLAB for data acquisition. The Caret library in R was used to perform KNN analyses. Validity of our estimator was performed with five-Fold Cross-Validation to all our experiments [26]. Code repository link in Supplementary Information (Section V).

### III. RESULTS

We focus on the CoP prediction done from skin afferent signals and compare them to predictions obtained from equivalent mechanisms (i.e., springs and string ligaments). For all the following results, unless explicitly mentioned, training and testing were done with the K-Nearest Neighbor approach described in Methods (Section II-B and II-C).

#### A. Double Stance Case

Skin wrapped around the ankles of a bipedal structure can be used to show its CoP location. In our experiments we estimate the location of the biped's CoP with a mean accuracy >81.5%.

**Four CoP locations experiments:** Force plate prediction accuracy for these experiments was 97.6%. Three tests were performed; for each tests, CoP values assigned by the force plate were predicted with respective accuracies: 87.44%, 82.76% and 77.29%. In Fig. 4-A the CoP prediction accuracy for one of the tests of this experiment is presented (i.e.,  $87.44\% = 97.6\% \times 89.6\%$ ).

**Nine CoP locations experiments:** Force plate prediction accuracy for this experiments was 97.2%. One tests was performed; the CoP values assigned by the force plate were predicted with an accuracy of: 80.8%. In Fig. 4-B the CoP prediction accuracy for this experiment is presented (i.e.,  $78.53\% = 97.2\% \times 80.8\%$ ).

#### B. Single Stance Case: Skin vs. Ligaments

For single stance case situations, ankle-wrapping skin or ligament strain afferent signals suffice on estimating the structure's CoP.

The mean prediction accuracy for the skin case was 91.44% while for the string and spring ligament cases was: 86.68% and 95.75% respectively (Table I). It is important to consider that skin sensors are not calibrated; this can be seen in (Fig. 3) when comparing section A (same baseline for all signals) with section B (different baseline for each signal), respectively for the skin and spring cases.

#### C. Single Stance Case: Skin with 30 and 40 mm Spring Leaf Sensor versions

Regardless of their type, sensors that provide strain measurements of ankle skin can enable CoP estimation. Here we show how similar CoP prediction results can be obtained from two versions of the used sensor.

**Nine CoP locations experiments:** When the CoP was estimated from the artificial skin afferent signals, the maximum and minimum prediction accuracies were 96.79% and 81.5% (Table I). For the skin, a total of 6 prediction accuracies were calculated using different leaf spring sensor sizes: 3 for the 30 mm and 3 for the 40 mm cases. Respectively, the mean prediction accuracies obtained were 87.42% and 95.47%.

**Sixteen CoP locations experiments:** For this case, the CoP was estimated with a mean prediction accuracy of 97.05% (Table I).

TABLE I  
CENTER OF PRESSURE PREDICTION ACCURACY, SINGLE STANCE

	min	max	median	
Afferent Signals	<b>Skin</b> (with 40 mm Leaf Spring Sensors)	0.93	0.97	0.96
	<b>Skin</b> (with 30 mm Leaf Spring Sensors)	0.81	0.94	0.87
	<b>Dacron Cable Ligaments</b>	0.85	0.89	0.86
	<b>Extension Spring Ligaments</b>	0.93	0.99	0.95
	<b>Skin with 30 mm Leaf Spring Sensor + Extension Spring Ligament</b> (Skin Stiffness << Spring Stiffness)	0.87	0.90	0.90
	<b>Skin with 30 mm Leaf Spring Sensor + Extension Spring Ligament</b> (Skin Stiffness < Spring Stiffness)	0.85	0.93	0.87
	<b>Skin</b> (with 30 mm Leaf Spring Sensors)	0.96	0.98	0.97
				16 CoPL
				9 Center of Pressure Locations (CoPL)

#### D. Single Stance Case: Skin and Ligament combination

Here we show how the CoP can be estimated using signals from skin and tendon strain sensors simultaneously (Fig 2 and Table I). Signals from different sensors are used to build a prediction or understanding of a phenomenon or parameter (see Discussion, Section IV).

Maximum and minimum CoP prediction accuracy values for these cases were 92.79% and 84.85%. Even though skin and extension spring elements have very different stiffnesses, we didn't observe a significant drop in prediction accuracy with respect to the other already presented results (Table I).

#### E. Statistical Significance

After performing a five-fold cross-validation to all our experiments, we obtained a Kappa value that was always above 0.81 for the single stance experiments. For the double stance experiments, we consistently obtained a Kappa value above 0.70. The obtained values point to a substantial or an near-perfect agreement (Kappa >0.61 or Kappa >0.81 respectively) [26]. Overall, this can be interpreted as the prediction almost always been accurate: the prediction "agrees" with the real or ground truth values.

#### F. Convergence to Stable Equilibrium Point

To demonstrate how the plant, for all skin and ligaments stance configurations, converges to a stable equilibrium point (i.e., neutral ankle position or foot-leg in a 90 deg angle), we let the ankle go to its neutral position after perturbing it. During this simple test we observed how signals converge to the same signal value (e.g. 1400 for the extension spring configuration).

A)

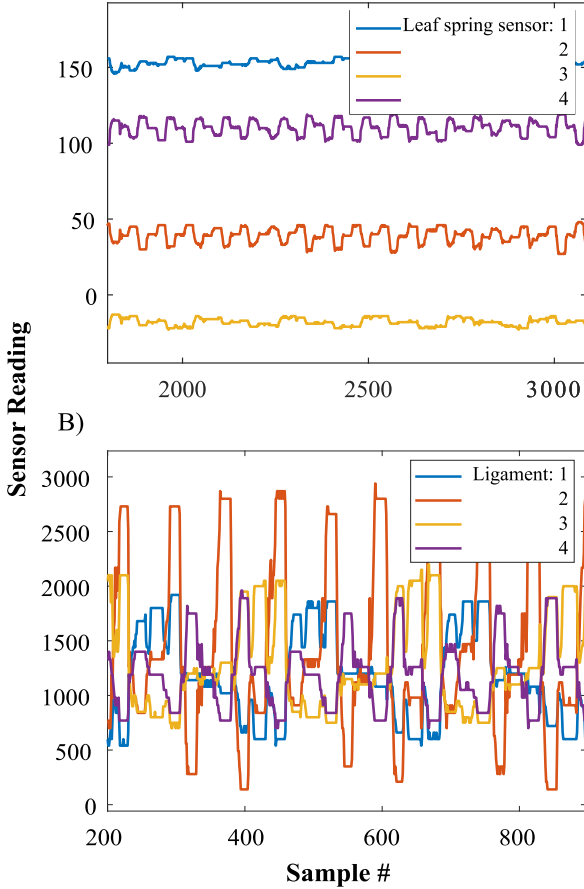


Fig. 3. **Raw signal samples:** A) Skin with 40 mm Leaf Spring and B) Extension Spring Ligaments.

#### IV. DISCUSSION

We show that bio-inspired proprioceptive skins and/or ligament arrangements can provide reliable COP predictions via a model-free machine learning approach (KNN), while permitting arbitrary postures of the ankle and no sensors on the sole of the foot prone to wear and damage. It is important to consider that we use a very low-cost artificial skin to show that different kinds of skins and/or ligaments (capable of measuring strain or longitudinal deformation) can be used to calculate the CoP. We propose this novel approach to estimate the CoP, that can be used to improve locomotion control in a new class of bio-inspired rigid, soft and hybrid (soft-rigid) legged robots.

Our work is motivated by the well-known problem that sensors placed on the sole of the foot are subject to wear and impulse forces [22]. Our alternative, as in nature, is to use skin and ligament strain sensors at the ankle. Our work now demonstrates that these non-collocated strain sensors suffice to estimate the CoP of bipeds during double and single stance. We observed that non-homogeneously distributed sensors, subjected to different conditions (i.e., strain sensors mounted on a combination of skin and ligaments surrounding the ankle, as described in Section III-D, Figure 2 and Table I) can enable the prediction of body states. This observation is aligned with our previous publication [27] where sensory signals are fused to show the benefits of distributed sensing for balance. Sensorized skins also have the advantages of (i) passively stabilizing the ankle, while (ii) not restricting the DoFs of the mechanism, allowing smooth movements and applicability to soft or hybrid (soft-rigid) robots [21].

Similar to our approach, in [18], the CoP location of a commercial prosthetic foot was estimated by measuring the strain experienced by structural elements at the ankle. We extend that approach by showing that measuring skin and ligament strain is also enough to calculate the CoP. Table I and Fig. 4 show that we can estimate the CoP for the double and single stance cases, mean prediction accuracy values of 92.4% and 81.51% respectively.

Even though we got a mean CoP prediction accuracy >80% in the double stance experiments, we identified two main areas for potential improvements of this experiment: (i) using a robotic biped with motors to change its posture, instead of manually changing and holding new positions and (ii) increasing the resolution of the force plate used to provide more accurate ground truth CoP values. As shown in Fig. 4-A and explained in Section II-B; our self-built force plate provides measurements of the ground truth for the four CoP locations to be predicted with skin afferent signals. But the resolution of the force plate may not have been high enough to provide accurate ground truth CoP locations for the nine CoP locations experiment (Fig. 4-B). This likely explains why we do not see a solid blue diagonal in Fig. 4-B. Regarding the ability of the skin alone to estimate the CoP, we show that (for the single stance experiments, where no force plate is involved) afferent signals from the skin suffice to estimate up to 16 CoP locations with a prediction accuracy

TABLE II

CENTER OF PRESSURE PREDICTION ACCURACY, SINGLE STANCE:  
"BLIND TESTS": VARIABLE AND UNKNOWN TRAINING LOAD

	min	max	median	
Afferent Signals				16 CoPL 9 Center of Pressure Locations (CoPL)
Skin (with 40 mm Leaf Spring Sensors)	0.74	0.94	0.79	
Skin (with 30 mm Leaf Spring Sensors)	0.73	0.84	0.82	
Dacron Cable Ligaments	0.92	0.95	0.94	
Extension Spring Ligament	0.92	0.97	0.93	
Skin with 30 mm Leaf Spring Sensor + Extension Spring Ligament (Skin Stiffness << Spring Stiffness)	0.76	0.84	0.82	
Skin with 30 mm Leaf Spring Sensor + Extension Spring Ligament (Skin Stiffness < Spring Stiffness)	0.71	0.87	0.80	
Skin (with 30 mm Leaf Spring Sensors)	0.81	0.85	0.83	

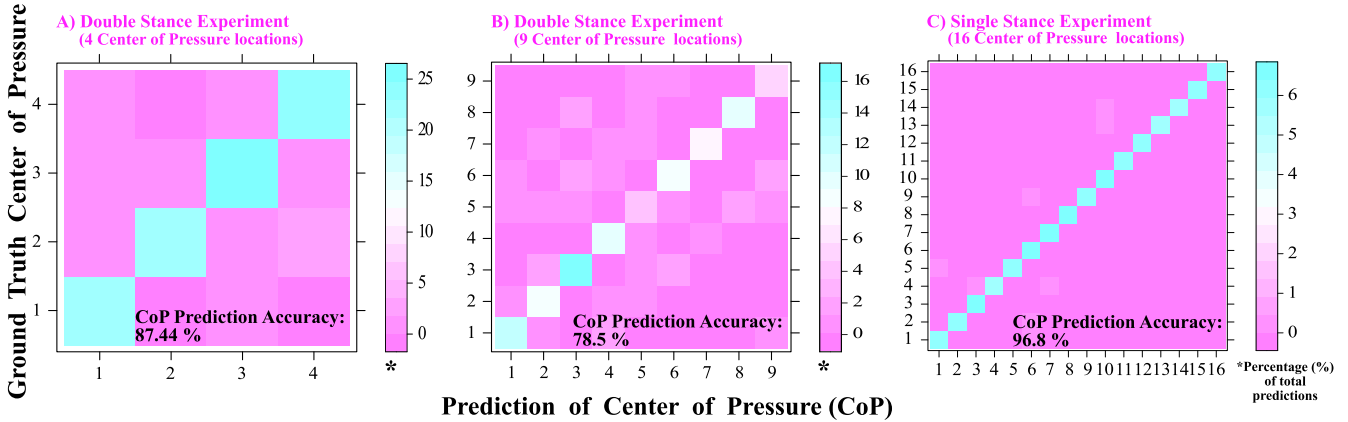


**Fig. 4. Skin strain afferent signals enable the prediction of the Center of Pressure.** Confusion Matrices that show percentages of how much the prediction of the CoP (i.e., x axis) agrees with the ground truth CoP value (i.e., y axis). All cases done using skin with 30 mm Leaf Spring Sensors. **A)** Double stance experiment, four CoP locations prediction accuracy:  $87.44\% = 97.6\% \times 89.6\%$ . 97.6% Force Plate Prediction Accuracy. CoP values assigned by the plate were 89.6% correctly predicted using skin afferent signals. **B)** Double stance experiment, nine CoP locations prediction accuracy:  $78.53\% = 97.2\% \times 80.8\%$  (Same rationale than in A). Even though this prediction value is high, CoP values were not assigned correctly by the force plate: the biped was manipulated to reach nine CoP locations (as described in Section II-B), but only some points (i.e., labels) were assigned by the plate while performing the task. This is considered a poor test due to the incapability of the force plate to better assign nine CoP location labels. **C)** We show with the single stance experiment that a synthetic skin is capable of providing signals to estimate 16 CoP values. Experiments protocol described in Section II-B and II-C and in Fig. 1-B.

of 96.8% (Fig. 4-C).

We did an additional ‘blind test’ which involves a training load with variable and unknown magnitude. This was our attempt to approximate what a foot would experience in a natural terrain where ground reaction forces are variable and not known *a priori*. We repeated the experiments described in the Section II-C and Fig. 1-B, but instead of applying a same 900g load, a human operator applied a variable and unmeasured load to the foot sole with her index finger at the same specified locations (results on Table II). We obtained overall prediction accuracies close to the ones obtained for the constant force case (cf. 84.53%, Table II, and 91.37%, Table I). Kappa Values consistently pointing to high prediction accuracy (i.e.,  $>0.61$  for setups combining skin and ligaments and  $>0.71$  for setups with only skin or ligaments).

Finally, the consistency of all results involving two versions of the spring-leaf skin sensors, ligaments, and skin+ligaments combination (Tables I, II and Fig. 4-C) highlights the likely generalizability of our approach to different kinds of artificial skins, ligaments and their combination. This approach should be useful to robotics, as it is known to be critical in biological systems. As mentioned in [28], afferent signals produced by skin stretched at the ankle or knee have a significant impact on the control of joint angles during walking. In [28], the importance of skin sensation is stressed by showing that it has a greater impact on ankle joint control than visual cues.

## V. CONCLUSIONS

We believe that this bio-inspired study will motivate engineers and scientists to further explore the benefits and applications of the bio-inspired, non-collocated proprioception for the control of locomotion in legged robots.

## SUPPLEMENTARY INFORMATION

The code and the supplementary files can be accessed through project’s Github repository at:

[https://github.com/CatStrain/Cat\\_skin](https://github.com/CatStrain/Cat_skin)

## ACKNOWLEDGMENTS

The authors thank Tailun Liu for his help on developing the first versions of the circuits used for the experiments, Suraj Chakravarthi Raja for helping in proofreading the manuscript. The authors acknowledge the access to equipment for building experimental hardware provided by the Baum Family Makerspace, from the Viterbi School of Engineering (USC). Research reported in this publication was supported in part by the Department of Defense CDMRP Grant MR150091, and Award W911NF1820264 from the DARPA-L2M program, as well as National Institutes of Health under the award number R21-NS113613 to F.J.V.-C. The authors acknowledge support for D.U.-M. by the research fellowship granted by Consejo Nacional de Ciencia y Tecnología (CONACYT-Mexico).

## REFERENCES

- [1] D. A. Kistemaker, A. J. K. Van Soest, J. D. Wong, I. Kurtzer, and P. L. Gribble, “Control of position and movement is simplified by combined muscle spindle and golgi tendon organ feedback,” *Journal of neurophysiology*, vol. 109, no. 4, pp. 1126–1139, 2013.
- [2] D. A. Hagen, A. Marjaninejad, and F. J. Valero-Cuevas, “A bio-inspired framework for joint angle estimation from non-collocated sensors in tendon-driven systems,” in *2020 IEEE International Conference on Intelligent Robots and Systems (IROS)*. IEEE, 2020.
- [3] R. M. Palmieri, C. D. Ingersoll, M. B. Stone, and B. A. Krause, “Center-of-pressure parameters used in the assessment of postural control,” *Journal of sport rehabilitation*, vol. 11, no. 1, pp. 51–66, 2002.
- [4] A. Drăgulinescu, A.-M. Drăgulinescu, G. Zincă, D. Bucur, V. Feies, and D.-M. Neagu, “Smart socks and in-shoe systems: State-of-the-art for two popular technologies for foot motion analysis, sports, and medical applications,” *Sensors*, vol. 20, no. 15, p. 4316, 2020.
- [5] U. Proske and S. C. Gandevia, “The proprioceptive senses: their roles in signaling body shape, body position and movement, and muscle force,” *Physiological reviews*, vol. 92, no. 4, pp. 1651–1697, 2012.

- [6] T. Yang, D. Xie, Z. Li, and H. Zhu, "Recent advances in wearable tactile sensors: Materials, sensing mechanisms, and device performance," *Materials Science and Engineering: R: Reports*, vol. 115, pp. 1–37, 2017.
- [7] H. Jörntell and C.-F. Ekerot, "Topographical organization of projections to cat motor cortex from nucleus interpositus anterior and forelimb skin," *The Journal of Physiology*, vol. 514, no. 2, pp. 551–566, 1999.
- [8] B. B. Edin, "Quantitative analyses of dynamic strain sensitivity in human skin mechanoreceptors," *Journal of neurophysiology*, vol. 92, no. 6, pp. 3233–3243, 2004.
- [9] B. B. Edin and N. Johansson, "Skin strain patterns provide kinaesthetic information to the human central nervous system." *The Journal of physiology*, vol. 487, no. 1, pp. 243–251, 1995.
- [10] R. L. Mildren, C. M. Hare, and L. R. Bent, "Cutaneous afferent feedback from the posterior ankle contributes to proprioception," *Neuroscience letters*, vol. 636, pp. 145–150, 2017.
- [11] C. R. Lowrey, N. D. Strzalkowski, and L. R. Bent, "Skin sensory information from the dorsum of the foot and ankle is necessary for kinesthesia at the ankle joint," *Neuroscience letters*, vol. 485, no. 1, pp. 6–10, 2010.
- [12] J.-M. Aimonetti, V. Hospod, J.-P. Roll, and E. Ribot-Ciscar, "Cutaneous afferents provide a neuronal population vector that encodes the orientation of human ankle movements," *The Journal of physiology*, vol. 580, no. 2, pp. 649–658, 2007.
- [13] V. Prahlad, G. Dip, and C. Meng-Hwee, "Disturbance rejection by online zmp compensation," *Robotica*, vol. 26, no. 1, pp. 9–17, 2008.
- [14] E. C. Martinez-Villalpando, H. Herr, and M. Farrell, "Estimation of ground reaction force and zero moment point on a powered ankle-foot prosthesis," in *2007 29th Annual International Conference of the IEEE Engineering in Medicine and Biology Society*. IEEE, 2007, pp. 4687–4692.
- [15] M. Folgheraiter, A. Yessaly, G. Kaliyev, A. Yskak, S. Yessirkepov, A. Oleinikov, and G. Gini, "Computational efficient balance control for a lightweight biped robot with sensor based zmp estimation," in *2018 IEEE-RAS 18th International Conference on Humanoid Robots (Humanoids)*. IEEE, 2018, pp. 232–237.
- [16] K. Erbatur, A. Okazaki, K. Obiya, T. Takahashi, and A. Kawamura, "A study on the zero moment point measurement for biped walking robots," in *7th International Workshop on Advanced Motion Control. Proceedings (Cat. No. 02TH8623)*. IEEE, 2002, pp. 431–436.
- [17] M. Shimojo, T. Araki, A. Ming, and M. Ishikawa, "A zmp sensor for a biped robot," in *Proceedings 2006 IEEE International Conference on Robotics and Automation, 2006. ICRA 2006*. IEEE, 2006, pp. 1200–1205.
- [18] S. Schütz, A. Nezhadfar, N. Dorosti, and K. Berns, "Exploiting the intrinsic deformation of a prosthetic foot to estimate the center of pressure and ground reaction force," *Bioinspiration & Biomimetics*, 2020.
- [19] M. Vukobratović and B. Borovac, "Zero-moment point—thirty five years of its life," *International journal of humanoid robotics*, vol. 1, no. 01, pp. 157–173, 2004.
- [20] M. Fliess and C. Join, "Model-free control," *International Journal of Control*, vol. 86, no. 12, pp. 2228–2252, 2013.
- [21] T. G. Thuruthel, B. Shih, C. Laschi, and M. T. Tolley, "Soft robot perception using embedded soft sensors and recurrent neural networks," *Science Robotics*, vol. 4, no. 26, 2019.
- [22] Z. Li, B. Vanderborght, N. G. Tsagarakis, L. Colasanto, and D. G. Caldwell, "Stabilization for the compliant humanoid robot coman exploiting intrinsic and controlled compliance," in *2012 IEEE International Conference on Robotics and Automation*. IEEE, 2012, pp. 2000–2006.
- [23] D. A. Winter, "Human balance and posture control during standing and walking," *Gait & posture*, vol. 3, no. 4, pp. 193–214, 1995.
- [24] B. J. Benda, P. O. Riley, and D. E. Krebs, "Biomechanical relationship between center of gravity and center of pressure during standing," *IEEE Transactions on Rehabilitation Engineering*, vol. 2, no. 1, pp. 3–10, 1994.
- [25] L. E. Peterson, "K-nearest neighbor," *Scholarpedia*, vol. 4, no. 2, p. 1883, 2009.
- [26] J. R. Landis and G. G. Koch, "The measurement of observer agreement for categorical data," *biometrics*, pp. 159–174, 1977.
- [27] D. Urbina-Meléndez, K. Jalaleddini, M. A. Daley, and F. J. Valero-Cuevas, "A physical model suggests that hip-localized balance sense in birds improves state estimation in perching: implications for bipedal robots," *Frontiers in Robotics and AI*, vol. 5, p. 38, 2018.
- [28] E. E. Howe, A. J. Toth, L. A. Vallis, and L. R. Bent, "Baseline skin information from the foot dorsum is used to control lower limb kinematics during level walking," *Experimental brain research*, vol. 233, no. 8, pp. 2477–2487, 2015.